

รายงานวิจัยฉบับสมบูรณ์

โครงการ

Structure-based mutagenesis and functional characterization of BinB from Lysinibacillus sphaericus

โดย

ดร.กนกพร ศรีสุจริตพานิช

รายงานวิจัยฉบับสมบูรณ์

โครงการ

Structure-based mutagenesis and functional characterization of BinB from Lysinibacillus sphaericus

ผู้วิจัย

ดร.กนกพร ศรีสุจริตพานิช

มหาวิทยาลัยบูรพา

สนับสนุนโดยสำนักงานกองทุนสนับสนุนการวิจัย และ มหาวิทยาลัยบูรพา

(ความเห็นในรายงานนี้เป็นของผู้วิจัยสกว. ไม่จำเป็นต้องเห็นด้วยเสมอไป)

บทคัดย่อ

รหัสโครงการ: MRG5980076

ชื่อโครงการ: Structure-based mutagenesis and functional characterization of BinB from *Lysinibacillus*

sphaericus

ชื่อหักวิจัย และสถาบัน: ดร.กนกพร ศรีสุจริตพานิช มหาวิทยาลัยบูรพา

อีเมล์: kanokporns@go.buu.ac.th

ระยะเวลาโครงการ: พฤษภาคม พ.ศ. 2559 – เมษายน พ.ศ. 2563

บทคัดย่อ:

โปรตีนสารพิษไบนารี่ที่ผลิตโดยแบคทีเรีย Lysinibacillus sphaericus (Ls) มีฤทธิในการฆ่าลูกน้ำยุงที่เป็น แมลงพาหะที่สำคัญ โครงสร้างของโปรตีนชนิดนี้มีลักษณะคล้ายกับโปรตีนสร้างรูรั่วในกลุ่มแอโรไลซิน โปรตีน สารพิษไบนารี่ ประกอบด้วยโปรตีน BinA และ BinB ที่ทำงานร่วมกันเพื่อฆ่าลูกน้ำยุง โปรตีน BinA และ BinB แสดง โครงสร้างที่คล้ายคลึงกับโปรตีนสร้างรูรั่วในกลุ่มแอโรไลซิน (Aerolysin) อย่างไรก็ตาม N-terminal โดเมน ที่ทำหน้าที่ จับจำเพาะจะมีความแตกต่างกันมากที่สุด จนถึงปัจจุบันการทำงานของกรดอะมิโนที่สำคัญใน N-terminal โดเมนของ โปรตีน BinB ยังไม่ทราบแน่ชัด ในการศึกษาครั้งนี้ กรดอะมิโนอะโรมาติกของโปรตีน BinB จะถูกแทนที่ด้วยอะลานีน เพื่อทดสอบฤทธิ์ทางชีวภาพของลูกน้ำยุง ผลการทดลองพบว่า Y72A และ Y111A ของ BinB มีความเป็นพิษลดลงเมื่อ เปรียบเทียบกับโปรตีน BinB ดั้งเดิม การทดสอบการจับจำเพาะแสดงให้เห็นว่า Y72A และ Y111A ของ BinB ลด สัญญาณการจับกับตัวรับในกระเพาะของลูกน้ำยุงโดยเทคนิค immunohistochemistry การจับกันของโปรตีน BinA และ BinB ถูกทดสอบโดยใช้ plasmon resonance (SPR) ฮิสทิดีนคอนจูเกต BinB สามารถเชื่อมติดกับ CM5 และแสดงให้ เห็นถึงการจับกันระหว่าง BinA กับ BinB อย่างไรก็ตามโปรตีน BinB กลายพันธุ์ ไม่สามารถผูกเข้ากับชิปเซ็นเซอร์ CM5 ได้ จากการศึกษาก่อนหน้าพบว่าโปรตีนสารพิษไบนารี่จับกับเยื่อหุ้มเซลล์ก่อนที่จะเกิดการออกฤทธิ์ เพื่อ ์ ตรวจสอบการมีปฏิสัมพันธ์กับเยื่อหุ้มเซลล์ โปรตีนสารพิษไบนารีฮิสทิดีนคอนจูเกตติดอยู่บนพื้นผิวของไขมัน bilayer ผ่านทาง Ni²+ chelating ประสบความสำเร็จในการจับกับ Ni²+-POPC/POPE bilayer (เลียนแบบเยื่อหุ้มเซลล์ยุง) แต่ ไม่ใช่สำหรับ Ni²⁺-POPC Bilayer อย่างไรก็ตามตรวจพบการจับกันที่ไม่เสถียรสำหรับ His-BinA เนื่องจากโปรตีนถูก ล้างด้วยบัฟเฟอร์ ในทางตรงกันข้าม His-BinB ทนต่อการล้างบัฟเฟอร์จนกว่าจะถูกแยกออกโดยสารละลาย imidazole N-terminal ที่โดเมนแตกต่างกันของสารพิษไบนารีได้รับการคาดว่าส่งผลต่อ His-Ni²⁺ chelating ของ His-BinA ยิ่งไป กว่านั้นการเปลี่ยนแปลงโครงสร้างระหว่างการเข้าใกล้ lipid membrane อาจลดประสิทธิภาพของ Ni²+ ที่มีผลผูกพันกับ His-BinA

คำหลัก: โปรตีนสารพิษไบนารี่, ลูกน้ำยุง, แบคทีเรีย *Lysinibacillus sphaericus*, SPR, Biacore

Abstract

Project Code: MRG5980076

Project Title: Structure-based mutagenesis and functional characterization of BinB from Lysinibacillus

Investigator: Dr.Kanokporn Srisucharitpanit, Burapha University

E-mail Address: kanokporns@go.buu.ac.th

Project Period: May 2017 - April 2020

Abstract:

Binary toxin is one of the bio-larvicidal toxin produced by Lysinibacillus sphaericus. BinA and BinB toxins are required together to exert its larvicidal activity. BinA and BinB proteins show a homology structure to pore forming-aerolysin family. However, N-terminal domain that act as a specific binding domain is the most different. To date, the function of critical amino acid in N-terminal domain of BinB is unavailable. Herein, aromatic residue of BinB will be replaced with alanine to test its biological activity on mosquito larvae. Y72A and Y111A of BinB showed significantly reduced toxicity when compare with wild type protein. Binding assay showed that Y72A and Y111A of BinB reduced binding signal in mosquito larval gut by immunohistochemistry. BinA and BinB interaction was performed using surface plasmon resonance (SPR). Histidine tagged BinB wild type could bind to CM5 sensor chip and showed binding activity to BinA. However, BinB mutant could not be achieve bind to CM5 sensor chip. Moreover, the binary toxin has been proposed to initial action on the susceptible cell membrane. To check interaction on membrane, the histidine-conjugated binary toxins were attached onto the lipid bilayer surface via Ni²⁺ chelating. Subsequently, the attachment was successful with Ni²⁺-POPC/POPE bilayer (mimic mosquito cell membrane) but not for Ni²⁺-POPC bilayer. However, unstable attachment was detected for His-BinA since bound protein could be removed by buffer rinsing. In contrast, His-BinB resisted to buffer rinsing until detaching by imidazole solution. The distinct N-terminal trefoil domain of binary toxin has been supposed to interfere the His-Ni2+ chelating of His-BinA. Moreover, structural conformational change during lipid membrane approaching may reduce the efficiency of Ni2+ binding of His-BinA.

Keywords: Binary toxin, Lysinibacillus sphaericus, Mosquito Iarvae, lipid membrane, SPR, Biacore

1. Introduction to the research problem and its significance

Mosquito-borne diseases are still a global health problem and cause human death especially in tropical countries. Aedes, Culex and Anopheles mosquito species are important vectors, or transmitters, of several infectious human diseases. For example, filariasis and Japanese encephalitis are transmitted by Culex spp., while malaria is transmitted by Anopheles spp. So, mosquito control is essential to reduce diseases distribution. The intensive use of chemical insecticides against vector mosquitoes has caused hazard to the environment and development of insecticide resistance. Therefore, to minimize use of chemical insecticides, the new perspectives have been opened since the discovery of microorganisms as a source of biological compounds for insect pest control. Mosquitocidal bacterial toxins are produced by Bacillus thuringiensis serovar israelensis (Bti) and Lysinibacillus (Bacillus) sphaericus. The highly toxic strains of L. sphaericus produce spore-associated crystalline inclusions classified as crystal toxin or binary toxin. L. sphaericus is one of the bacteria used as a bio-insecticide in the field and commercial products are currently available, for example, VectoLex and Spherimos. The advantages of using L. sphaericus in the mosquito control program include the persistence of the L. sphaericus bacteria in polluted water, which is a breeding preference for Culex larvae, and the longer existence of the binary toxin than toxins from B. thuringiensis subsp. Israelensis. However, the long term use of the binary toxin develops insect resistance to the binary toxin which has been reported in both laboratoryselected and field-treated populations. The mosquito resistance to binary toxin is dependent on multiple factors, for example, genetic background of the mosquito population, treatment strategy and population dynamics. Because the binary toxin binds specifically to a single class of receptor, the major cause of resistance involves in the disruption of receptor on larval gut endothelium, resulting in binding and toxicity failures. To prevent the risk of resistance, it is thus important to understand the nature and mechanism of action of the binary toxin.

Two major components of binary toxin named BinA and BinB function together to kill the mosquito larvae. The maximum larvicidal activity is achieved when they are present in a 1:1 M ratio of BinA and BinB, suggesting that it works as a binary toxin or AB toxin. BinA acts as a toxicity subunit and BinB provides a specific binding on epithelial membrane receptor. Recently, the structure of BinB has been elucidated by X-ray crystallographic technique. The BinB structure belongs to aerolysin-type β -pore forming toxin and is assigned into two domains, N-terminal and C-terminal domains. The N-terminal domain contains a β -trefoil fold which has a pseudo 3-fold rotation axis and a high conserve of folding with sugar binding proteins or lectins. The C-terminal domain is homologous to β -pore forming toxins. Based on atomic structure of BinB, we thus hypothesized that the N-terminal domain is a receptor-binding domain while the C-terminal domain is a translocation domain via pore formation. In this study, in order to provide deeper insights into the molecular mechanism of action of BinB, we will perform structure-based mutagenesis. We will firstly focus on BinB-NTD receptor-binding function. The critical amino acids for the larvicidal activity and receptor recognition will be investigated using both biological and biochemical assays.

Amino acid sequences of BinA and BinB show low homology to those of other bacterial toxins but high homology is observed among them with 25% identify and 40% similarity implying a similar folding structure [13]. Recently, three-dimensional structure of BinA and BinB proteins was resolved and it reveals a very high homology structure between them (Figure 1). The N-terminal domain is highly conserved to some sugar binding proteins whereas the C-terminal domain rich in β -sheets is similar to aerolysin toxins, a β -pore forming toxin [14,15]. Besides protein structure prediction, the function of each domain is necessary to be determined with experimental procedure. However, the studies of binary toxin have been limited because of its protein receptor requirement. Due to its proposed toxic mechanism of pore formation and cell internalization, the binary toxin has been supposed to function on cell membrane. In this work, the binary toxin has been attempted to bind on the lipid membrane surface via DGS-NTA(Ni2+) to mimic its binding on the target cell surface. The lipid bilayer environment may provide a suitable model system for studying BinA-BinB interaction and protein complex formation. The results showed that although Bin toxins share protein folding structure but their binding capacity of His-NTA(Ni2+) on both matrix column and lipid bilayer were different. His-BinB interacts with Ni2+-ion stronger than His-BinA. For future work, histidine tag will directly conjugate into the protease-activated BinA and BinB in order to determine its function under lipid bilayer condition.

2. Objectives

The ultimate objective of this study is to gain insights into molecular mechanism of the BinB protein by structure-based site-directed mutagenesis with following specific objectives:

- 1. To construct BinB mutant plasmids by site-directed mutagenesis.
- 2. To express BinB mutant proteins.
- 3. To characterize the critical amino acids for the larvicidal activity and receptor recognition *in vitro* by immunolocalization assay.
 - 4. To analyze carbohydrate-binding specificity and membrane lipid binding of BinB protein.

3. Methodology

3.1 Construction of BinB mutant plasmids

The pET28b-BinB plasmid, expressing (His)₆-tagged BinB protein, will be used as a template for generating the BinB mutant plasmids. Aromatic amino acid at N-terminal domain will be selected based on 3D structure of BinB. The selected amino acids will be replaced by alanine using complementary oligonucleotide primers containing the required mutations. All mutant plasmids will be generated following the procedure of the QuikChange™ site-directed mutagenesis method (Stratagene). PCR products will be treated with *DpnI* to

destroy the wild-type template and will be transformed to *E. coli* JM109 for mutant screening. All mutant plasmids will be confirmed by automate DNA sequencing before re-transforming to *E. coli* BL21(DE3)pLysS, the expression host cells.

3.2 Expression of BinB mutant proteins

Each recombinant *E. coli* BL21 (DE3) pLysS harboring mutant plasmids will be grown at 37 °C in a Luria-Bertani medium containing 50 μ g/ml kanamycin and 34 μ g/ml chloramphenicol until the OD₆₀₀ of culture reached 0.7. Then 0.2 mM of isopropyl- β -D-thiogalactopyranoside (IPTG) will be added to induce protein expression at 18 °C for 5 hours. Protein concentration of the protein will be determined by the method of Bradford using Bio-Rad protein assay reagent with bovine serum albumin as a standard. The BinB protein will be analyzed on sodium dodecyl sulfate polyacrylamide gel eletrophoresis (SDS-PAGE) compare with protein standard marker. The BinA protein will be expressed in order to use in mosquito larvicidal activity assay.

3.3 Mosquito-larvicidal activity assay

Bioassay for mosquito-larvicidal activity will be performed by using the 2^{nd} –instar *Culex quinquefasciatus* larvae. The BinB wild type only will be used as a negative control. The mixtures of BinB wild type and BinA at equimolar ratios will be diluted in distilled water (2-fold serial dilution). Then, 1 ml of each concentration of toxin will be added into 24-well plates containing 10 larvae/well in 1 ml DW (done in duplicate). Mortality will be recorded after incubation at room temperature for 48 h. All of the data from three independent experiments will be used to calculate median lethal concentration (LC_{50}) by using GWbasic program Probit analysis (Finney, 1971). All mutant proteins will be done as following the same method of wild type.

3.4 Purification of recombinant protein toxin

Supernatant from expressed cell lysate will be collected for protein purification by histidine affinity chromatography. The bound (His)₆-tagged BinB will be eluted with elution buffer containing 250 mM imidazole. The protein-containing fractions will be pooled and concentrated by ultrafiltration at 4°C using a Centriprep column (30-kDa cutoff, Amicon), followed by applying the concentrated pool into a Superdex 200 HR 10/30 column (GE Healthcare Life Sciences) which was equilibrated with 50 mM Tris-HCl, pH 9.0, and 1 mM DTT. The proteins collected at every step were analyzed by 12% sodium dodecyl sulfate- polyacrylamide gel electrophoresis (SDS-PAGE).

3.5 Circular dichroism

The secondary structures of the mutant BinB proteins will be determined by using a Jasco J-715 CD spectropolarimeter (Jasco Inc., USA). The CD spectra of the purified protein at a concentration of 1 mg/ml in

a quartz cuvette (0.2 mm optical path length) will be measured from 200 to 260 nm with scanning speed of 50 nm/min. Each spectrum will be averaged from three scans and a baseline subtracted. All spectrum of mutant protein will be compare with wild type protein.

3.6 Immunolocalization In vitro binding assays

The 4th-instar *C. quinquefasciatus* will be sectioned and immunohistochemical detection will be performed following a method described previously (Singkhamanan, *et al.*, 2010, Singkhamanan, *et al.*, 2013). The sections will be covered with the purified BinB, wild-type or mutant proteins for 45 min. The unbound proteins will be removed by washing three times in PBS, for 15 min each time. The bound toxin will be incubated with rabbit antiserum specific to BinB (1:10 000) for 45 min. After washing three times with PBS, biotin-goat antirabbit IgG (1:200) (Invitrogen) will be added and further incubated for 45 min. The slides will be washed three times with PBS and covered with HRP–streptavidin conjugate (1:500) (Invitrogen) for 45 min. The immune-complexes will be detected by incubation with 3, 30-diaminobenzidine (SK-400, Vector) for 2 min and the reaction will be stopped by rinsing with distilled water. The positive staining of the bound toxin will be indicated by the brown staining after analyzed under a light microscope.

3.7 Surface plasmon resonance (SPR) experiments

All surface plasmon resonance (SPR) experiments were performed in PBS (pH 7.4) at 25 $^{\circ}$ C using a BIAcore T200 instrument (GE Healthcare) at a flow rate of 30 μ L/min. To measure the affinities of BinA and BinB, the activated BinB was immobilized on a CM5 sensor chip (GE Healthcare) using an Amine Coupling Kit (GE Healthcare), resulting in a surface density of approximately 10000 resonance units (RU). Regeneration was achieved with 10mM glycine-HCl (pH 1.5). The binding kinetics were analyzed with BIAevaluation software, version 3.0, using the 1:1 binding model.

3.8 Sugar recognition site determination by soaking experiment

The native crystal of activated BinB will be prepared for soaking experiments following the previous crystallization study. Sugars will be selected to test for their binding with the BinB subunit. The soaking solution will be prepared by adding each sugar into the mother liquor with a final concentration of 100 mM. The activated BinB crystals will be soaked in sugars for 1 hour and then put in cryoprotectant before cryocooling to liquid nitrogen stream. X-ray diffraction data collection will be performed using the syncrhotron X-ray source (Synchrotron Light Research Institute, Thailand). Electron density maps will be calculated by molecular replacement method using the native structure of activated BinB as a search model. Sugar ligand coordinate obtained from the Protein Data Base will be manually fixed into the map.

3.9 Lipid vesicle preparation and characterization

1-palmitoyl,2-oleoyl-sn-glycero-3-phosphocholine (POPC) and 1-palmitoyl-2-oleoyl-sn-glycero-3-phosphoethanolamine (POPE) were purchased from Sigma-Aldrich. 1,2-dioleoyl-sn-glycero-3-[(N-(5-amino-1-carboxypentyl)iminodiacetic acid)succinyl] (DGS-NTA(Ni²⁺) was purchased from Avanti. All lipids were aliquot and stored at -20°C.

The desired molar ratio of lipid mixtures was mixed in chloroform. Lipid films were formed by evaporating the organic solvent under a gentle nitrogen stream for at least 1 hour. The lipid films were hydrated above the melting transition temperature (T_m) for 2 hours with TBS. The hydrated film was intermittently vortexed during incubation until complete suspension. The vesicles were homogenized by tip sonication with 50% duty cycle of 10 minutes (Branson sonifier). Then, the residual material was removed by centrifugation at 10,000g for 10 minutes. For pure POPC, the vesicles were repeatedly pressed through a polycarbonate membrane with a pore diameter of 50 nm by using a mini-extruder (Avanti). Before use, the vesicles size was determined by Zetasizer Nano ZS (Malvern Instrument). The vesicle solutions were stored at a temperature higher than T_m and were used within a week.

3.10 Quartz Crystal Microbalance with Dissipation (QCM-D) measurement

QCM-D experiments were carried out with Q-Sense E4 (Biolin Scientific). Lipid bilayer formation and further determination of Bin toxin-lipid interaction were performed on top of SiO_2 -coated sensor (QSX 303, Biolin Scientific). The sensors were sequentially cleaned with following steps of sonication in 2% (w/w) SDS solution for 15 minutes and rinsing with ultrapure water (MilliQ, Merck). Then, the sensors were dried under nitrogen stream. The sensors were finally treated with UV/Ozone cleaner (Bioforce Nanosciences) for 30 minutes. The fundamental frequency (5 Hz) and the frequencies of the overtones (3, 5, 7, 9, 11, and 13) were evaluated prior running the experiment. The changes in frequency (Δ F) and dissipation (Δ D) values were presented in this work correspond to the 5th overtone unless otherwise stated.

To form lipid bilayers, the QCM-D sensors were incubated with TBS under flow condition with a flow rate of 50 μ l/min until reach to a stable baseline (at least 1 hour). Then, 0.1 mg/ml lipid vesicle solutions were slowly filled into the QCM-D chamber with flow rate of 50 μ l/min. The lipid bilayer formation was indicated by changes of Δ F and Δ D values. After that, the excess vesicle was removed by buffer rinsing until reaching a stable baseline. The binary toxins were introduced into the system at flow rate of 50 μ l/min and then the flow was paused for protein binding until the signals were stable. The His-Bin toxins were eluted from Ni²⁺-lipid bilayer by imidazole containing TBS solution at the flow rate of 50 μ l/min. The experiments were carried out at 25 °C.

4. Results and discussion

4.1 BinA and BinB Structure comparison

In comparison, both BinA (PDB no.5foz) and BinB (PDB no.3wa1) structure composes of N-terminal and C-terminal domain which have similarity approximately 30% Z (Figure 4-1,2). The most different domain was N-terminal domain (NTD, Figure 4-3). The amino acid alignment of NTD represented four different regions as shown in figure 4-4. Structural based site directed mutagenesis was done based on 4 different regions of BinB. BinB have total aromatic amino acid of 26 residues composed of 14 Tyrosine and 12 Phenylalanine residues. In this study, Y48, Y53, Y72, Y76, Y94, Y111 and Y140 of BinB were selected to replace with alanine due to its side chain outside of the structure. The mutated positions in BinB was showed in figure 4-5.

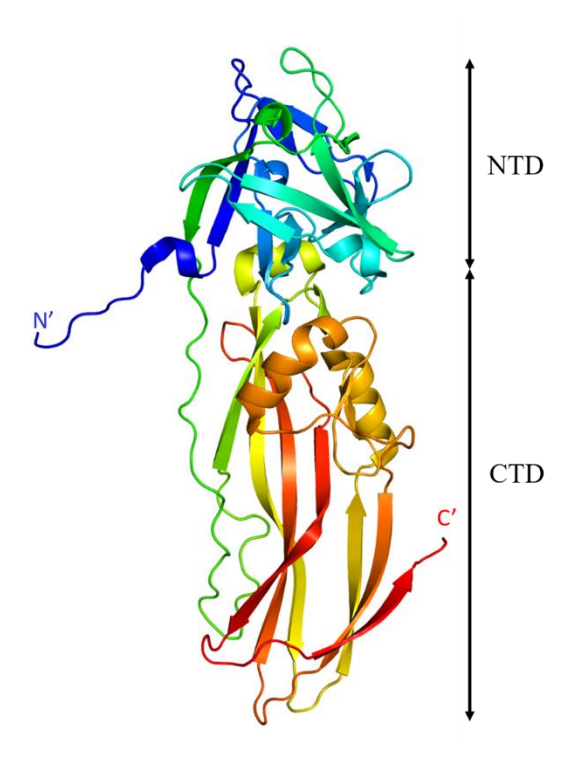


Figure 4-1 3D structure of BinA (PDB no.5foz) composes of N-terminal domain and C-terminal domain.

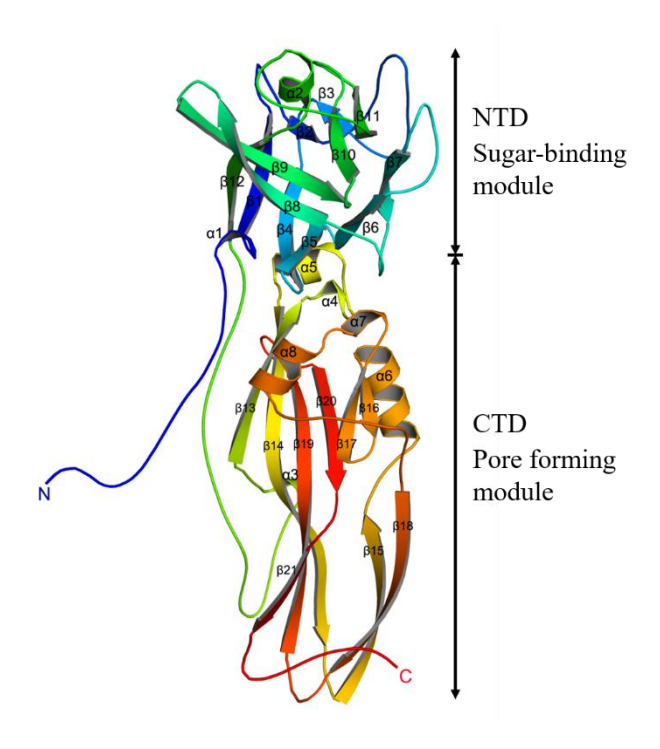


Figure 4-2 3D structure of BinB (PDB no.3wa1) composes of N-terminal domain and C-terminal domain

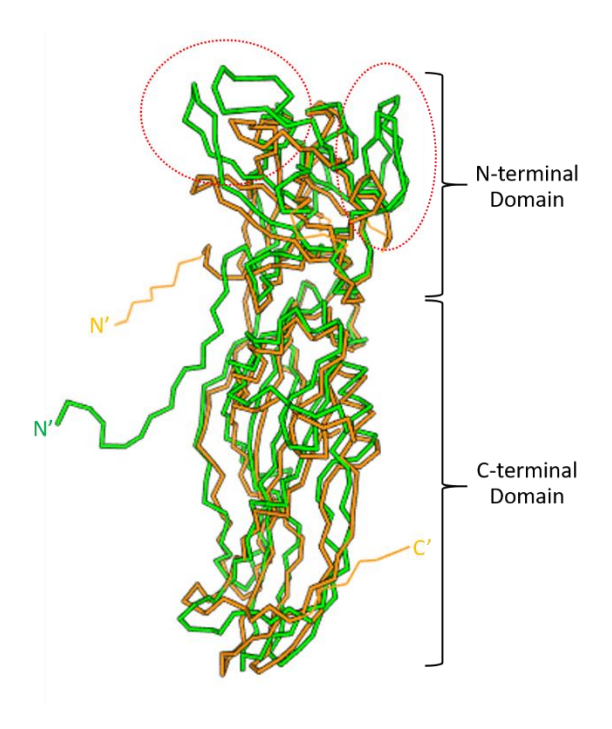


Figure 4-3 3D structure alignment of BinA and BinB using DALI server



Figure 4-4 amino acid sequence and secondary structure alignment of BinA and BinB showed 4 different regions as in red box.

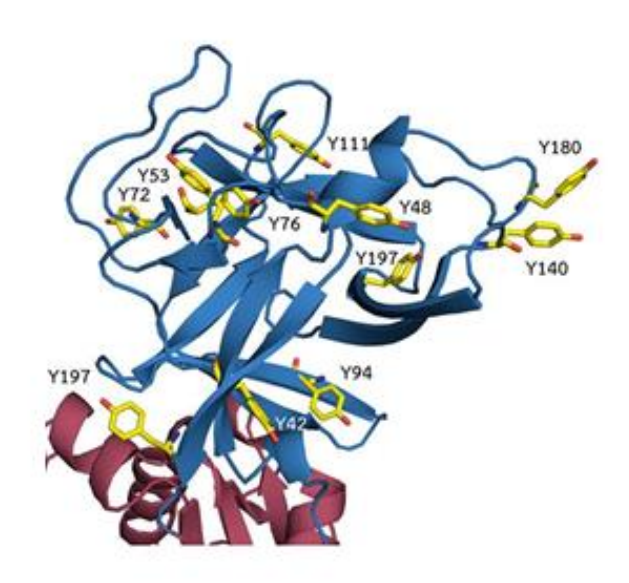


Figure 4-5 Tyrosine position of BinB as yellow stick.

4.2 Site directed mutagenesis

To determine the effect of mutations of these binding residues on the toxicity, tyrosin 48, 53, 72, 76, 94, 111 and 140 were replaced with alanine. The pET28b-BinB was used as a template for preparing mutant plasmids of Y48A, Y53A, Y72A, Y76A, Y94A, Y111A and Y140A. The mutagenic primers and their restriction sites are shown in Table 4-1. All PCR products were obtained following the thermal cycles and the annealing temperature (Ta) as 50°C. The amplified products and *DpnI* digested PCR products showed major bands of 6.6 kb, corresponding to the size of pET28b-BinB (Figure 4-7 and 4-8). Then, all *DpnI* digested PCR products were transformed into *E.coli* JM109 and the mutants screening were performed by restriction endonuclease analysis. The mutant plasmids were confirmed by DNA sequencing using T7 promoter and T7 terminator as sequencing primers (Figures 4-9).

Table 4-1 List of mutagenic primers and their restriction sites of BinB mutants

The letter f and r represent forward and reverse primers, respectively. The recognition sites for restriction enzyme analysis are underlined and mutated nucleotides are shown in bold.

Primer	Primer sequence	TM	bp	Rest Enz
Y 48 Af	5'-CCTTAAGAATA <mark>AA<u>GCT</u>T</mark> CACGGAATGG-3'	56.1	27 bp	HindIII
Y 48 Ar	5'-CCATTCCGTGA <u>AGC</u> TTTATTCTTAAGG-3'	56.1	27 bp	AAGCTT
Y 53 Af	5'-CACGG AATGGT <mark>GCA</mark> GGTTTATCAAAAACC-3'	60	29 bp	BspMI
Y 53 Ar	5'-GGTTTTTGATAAACC <u>TGC</u> ACCATTCCGTG-3'	60	29 bp	GCAGGT
Y 72 Af	5'-CCCATCTAACGA <mark>AGCT</mark> TCAATAATGTATGA-3'	57	30 bp	HindIII
Y 72 Ar	5'-TCATACATTATTGAAGCTTCGTTAGATGGG-3'	57	30 bp	AGCTT
Y 76 Af	5'-CGAATATTCAATAAT <mark>GGCC</mark> GATAATAAAGATC-3'	57	32 bp	Haelll
Y 76 Ar	5'-GATCTTTATTATC <u>GGC</u> CATTATTGAATATTCG-3'	57	32 bp	GGCC
Y 94 Af	5'-GATGATGGTAG <mark>AGCT</mark> ATTATTGCAGATAGAG-3'	59	31 bp	Alul
Y 94 Ar	5'-CTCTATCTGCAATAATAGCTCTACCATCATC-3'	59	31 bp	AGCT
Y 111 Af	5'-GCACCTAC <mark>T<u>GCA</u>TTGGATAATAACAATCACC-3'</mark>	60	31 bp	HpyCH4V
Y 111 Ar	5'-GGTGATTGTTATTATCCAA <u>TGC</u> AGTAGGTGC-3'	60	31 bp	TGCA
Y 140 Af	5'-GGTAGGTAGTGGA <mark>GAT<u>GC</u>T</mark> ATTACGGG-3'	61	27 bp	SfaNI
Y 140 Ar	5'-CCCGTAATAGCATCTCCACTACCTACC-3'	61	27 bp	GATGC

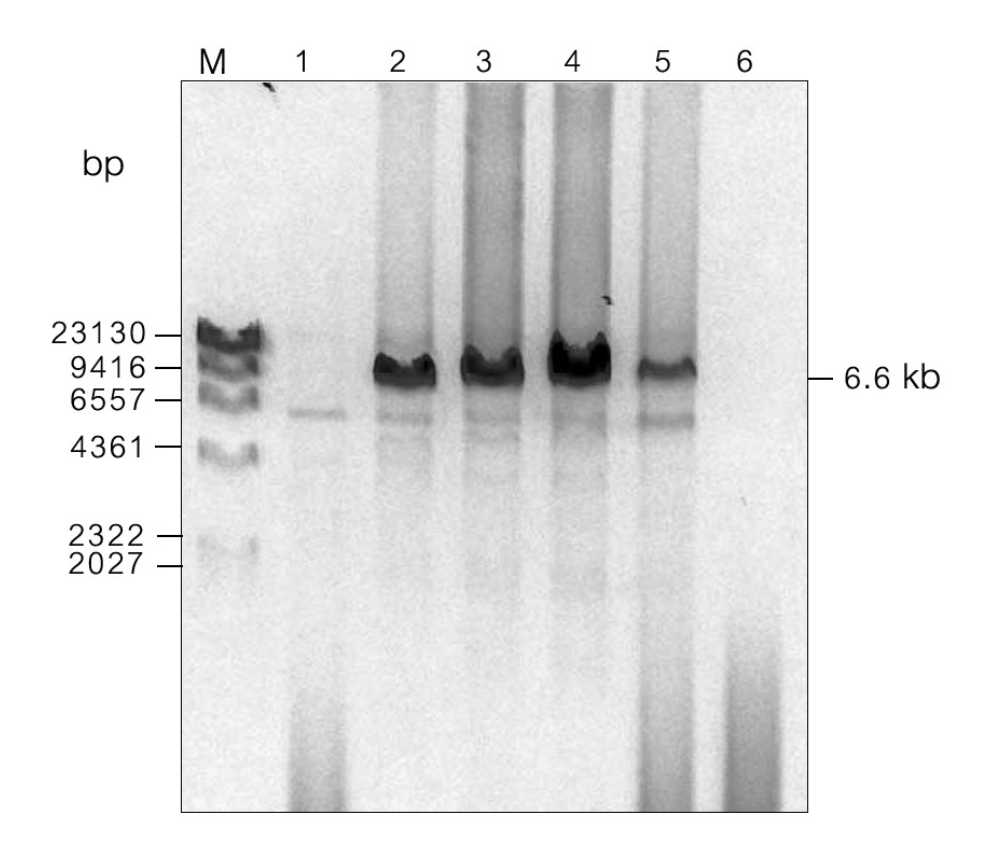


Figure 4-7 1% agarose gel electrophoresis of PCR product from site-directed mutagenesis

Lane M: Lamda HindIII DNA marker

Lane 1: Negative control

Lane 2: pET28b-BinB_Y48A

Lane 3: pET28b-BinB_Y72A

Lane 4: pET28b-BinB_F83A

Lane 5: pET28b-BinB_Y180A

Lane 6: negative control

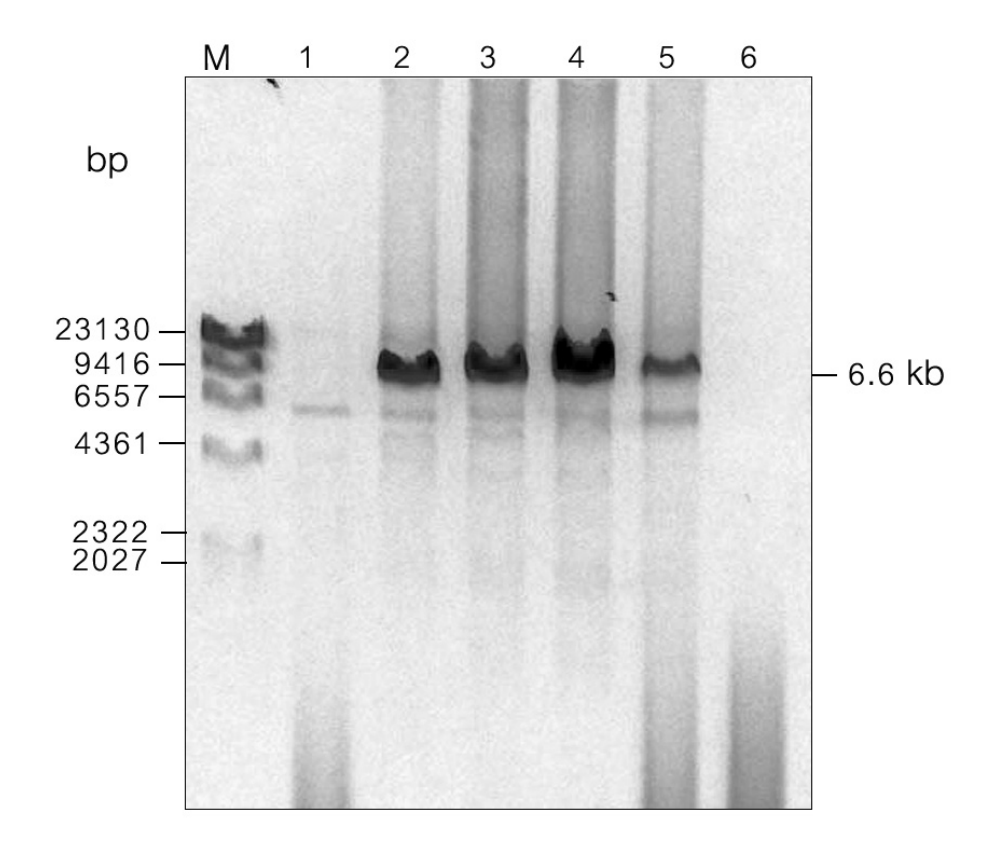


Figure 4-8 1% agarose gel electrophoresis of PCR product from site-directed mutagenesis

Lane M: marker HindIII DNA

Lane 1: pET28b-BinB_Y53A

Lane 2: pET28b-BinB_Y76A

Lane 3: pET28b-BinB_Y94A

Lane 4: pET28b-BinB_Y111A

Lane 5: pET28b-BinB_Y140A

Lane 6: pET28b-BinB Y140A (Negative control)

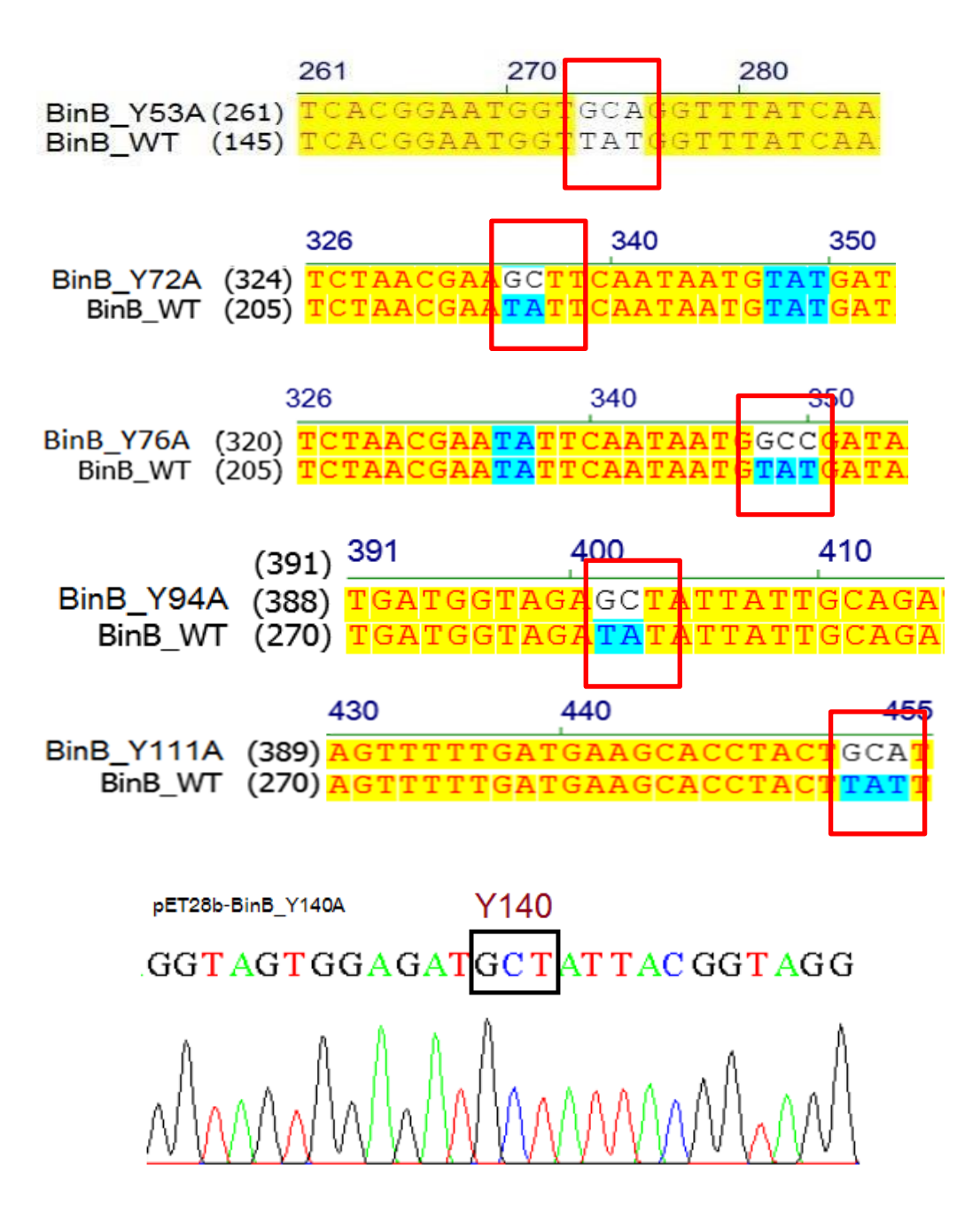


Figure 4-9 DNA sequencing analysis of pET28b-BinB_Y53A, pET28b-BinB_Y72A, pET28b-BinB_Y76A pET28b-BinB_Y94A, pET28b-BinB_Y111A and pET28b-BinB_Y140A

4.3 Expression and purification of BinB mutant proteins

 $\it E.coli$ cells harboring pET28b-BinB of each mutant plasmid were grown in Luria-Bertani (LB) medium containing 50 μg/ml kanamycin and 34 μg/ml chloramphenicol. The cultured cells were induced with 0.2 mM isopropyl $\it β$ -D thiogalactopyranoside (IPTG). The proteins were purified by histidine affinity chromatography. Non-specifically bound proteins were washed twice with wash buffer containing 25 mM imidazole and 50 mM imidazole, respectively. The bound (His)6-tagged BinB was eluted with elution buffer containing 100 mM imidazole. The imidazole was removed by desalting column (GE Healthcare Life Sciences) which was equilibrated with 50 mM Tris-HCl, pH 9.0. The proteins collected at every step were analyzed by 10% sodium dodecyl sulfate- polyacrylamide gel electrophoresis (SDS-PAGE). The purified proteins were shown in figure 4-10.

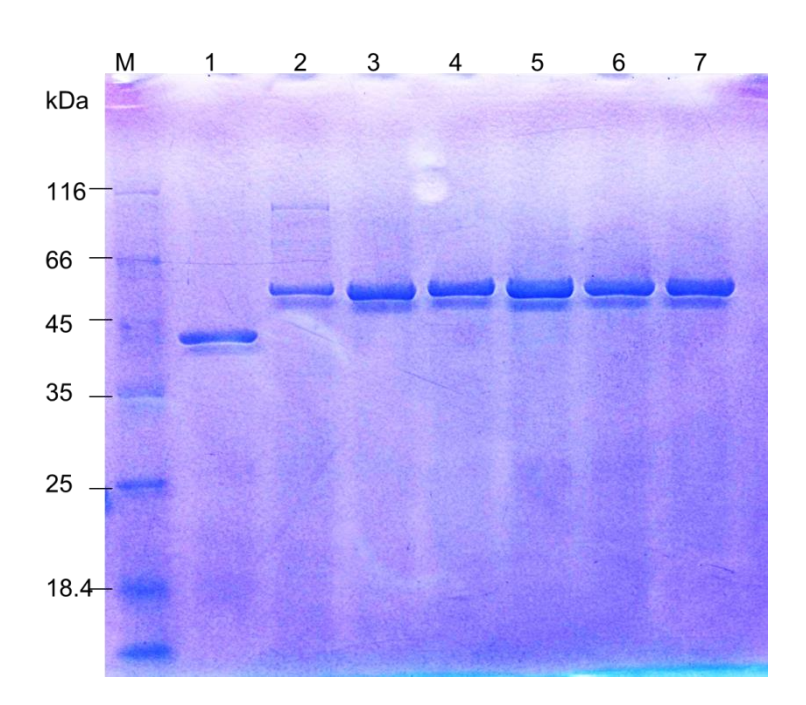


Figure 4-10. SDS PAGE analysis of purified proteins

Lane 1	Purified BinA protein
Lane 2	Purified wild type BinB protein
Lane 3	Purified mutant BinB Y53A protein
Lane 4	Purified mutant BinB Y72A protein
Lane 5	Purified mutant BinB Y76A protein
Lane 6	Purified mutant BinB Y94A protein
Lane7	Purified mutant BinB Y111A protein

4.4 Mosquito-larvicidal activity assay

Purified BinA and BinB were mixed at a 1:1 molar ratio, then 2-fold serially diluted with distilled water in different concentrations. Then, 1 ml of each protein dilution was added to each well of a 24-well tissue culture plate containing 10 larvae/well in 1 ml water. The BinB wild-type only was used as a negative control. The mutants BinB were mixed with BinA-wild type at a 1:1 molar ratio as same as protocol with wild type protein. Mortality was recorded after incubation at room temperature for 48 hours. All of the data from three independent experiments were used to calculate motility. The results are shown in Table 4-2. Of these mutants, Y53A, Y72A, Y76A and Y94A exhibited significant reduced larvicidal activity.

Table 4-2 Mosquito-larvicidal activity assay

Protein	LC ₅₀ * (μg/ml)	% Mortality conc.0.5 μg/ml	
BinA	NA	43.3	
BinB	Inactive	0	
BinA + BinB wild type	0.169	77.5	
BinA + Y53A	0.030	63.3	
BinA + Y72A	0.534	53.3	
BinA + Y76A	NA	50	
BinA + Y94A	0.236	63.3	
BinA + Y111A	0.107	82.5	
BinA + Y140A	NA	100	

^{*} The LC₅₀ (median lethal concentration) was calculated from three independent experiments by using Probit analysis.

4.5 Circular dichroism

The secondary structures of the recombinant BinA, BinB and mutant BinB proteins were determined by using a Jasco J-815 CD spectropolarimeter (Jasco Inc., USA). The CD spectra of the purified protein at a concentration of 1 mg/ml in a quartz cuvette (0.2 mm optical path length) was measured from 200 to 260 nm with scanning speed of 50 nm/min. Each spectrum was averaged from three scans and a baseline subtracted. The result as shown in figure 4-11. CD spectra in a far UV region (190-260 nm) of all mutants were similar to that of the wild-type protein.

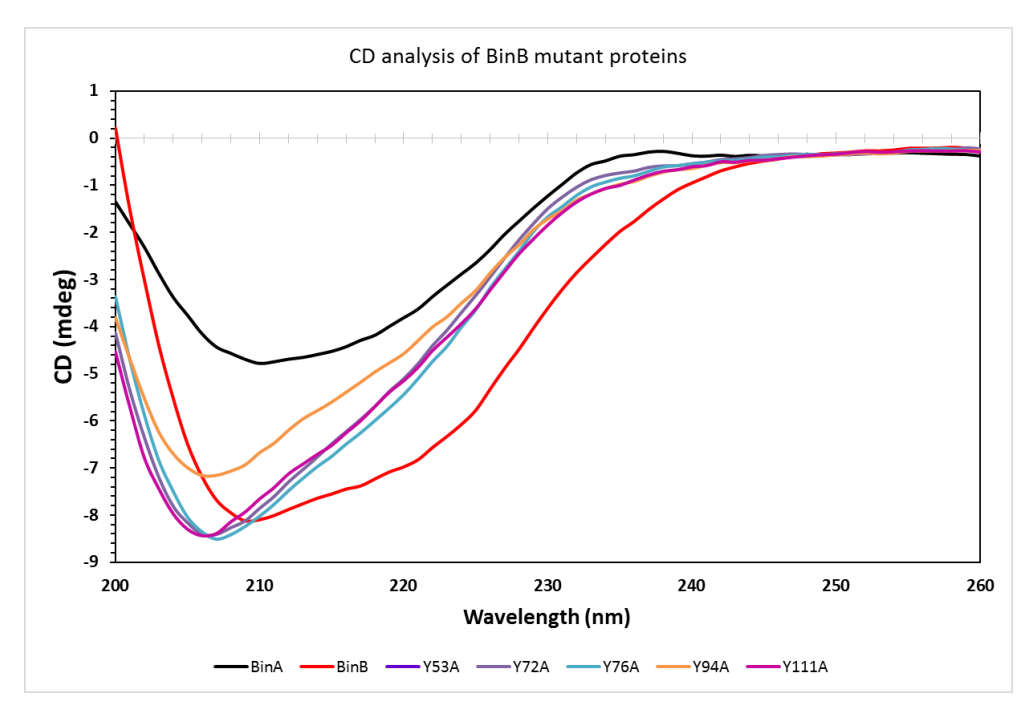


Figure 4-11. CD spectra of all mutant proteins

Base on structure of BinB, seven tyrosine residues at N-terminal domain of BinB were tyrosine 48, 53, 72, 76, 94, 111 and 140 which were selected to replace with alanine. All of mutant BinB proteins were successfully generated and were confirmed by DNA sequencing. The mutant toxins were expressed and purified following the same protocol as that of the wide-type toxin. Then the mutant proteins were tested the function using mosquito-larvicidal activity assay. Of these mutants, Y53A, Y72A, Y76A and Y94A exhibited significant reduced larvicidal activity. The secondary structure of mutants were analyzed by circular dichroism. CD spectra in a far UV region (190-260 nm) of all mutants were similar to that of the wild-type protein. In further investigation, we will find the critical residues involve in epithelial membrane interaction by immunolocalization. Additionary, sugar binding assay will be performed.

4.6 Immunohistochemistry for binding analysis of mutant protein

จากผลการทดสอบความเป็นพิษต่อลูกน้ำยุง ผู้วิจัยเลือกโปรตีนกลายพันธุ์ที่มีความเป็นพิษลดลงมาศึกษาการ จับกับ receptor ที่อยู่บน microvilli ในกระเพาะลูกน้ำยุง โดยทำการเตรียม section ลูกน้ำยุง นำมาเติมโปรตีนแต่ละตัว ดูการจับกันด้วยการย้อม Immunohistochemistry จะพบว่า BinB wild type negative control จะติดสีน้ำตาลจาง ๆ เนื่องจากในขั้นตอนการย้อมไม่ได้เติม primary antibody ลงไปจึงทำให้ได้รับสัญญาณจางๆ ในขณะที่ BinB wild type พบว่ามีการติดสีที่เข้มบริเวณ microvilli เมื่อเทียบกับ negative control นอกจากนี้ในส่วนของ BinB mutant ได้แก่ Y72A และ Y111A พบว่าติดสีจางกว่า BinB wild type เป็นไปได้ว่ามีบทบาทสำคัญในขั้นตอนการจับกับ receptor ทำ ให้ความเป็นพิษลดลง ดังแสดงในภาพที่ 4-12

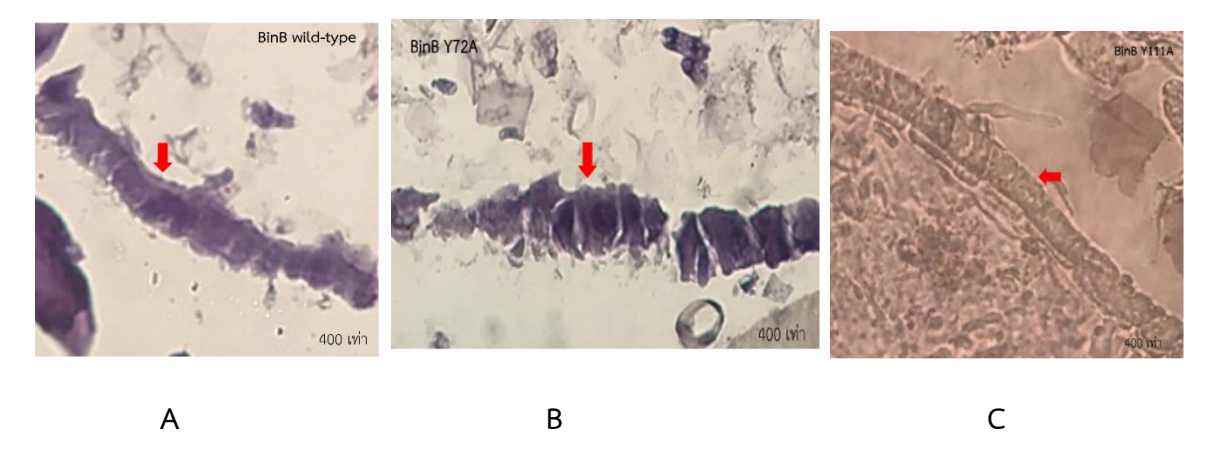


Figure 4-12 Immunohistochemistry of BinB mutant

A: BinB wild type (Positive)

B: BinB Y72A

C: BinB Y111A

4.7 surface plasmon resonance (SPR)

All surface plasmon resonance (SPR) experiments were performed in PBS (pH 7.4) at 25 $^{\circ}$ C using a BIAcore T200 instrument (GE Healthcare) at a flow rate of 30 μ L/min. To measure the affinities of BinA and BinB, the activated BinB was immobilized on a CM5 sensor chip (GE Healthcare) using an Amine Coupling Kit (GE Healthcare), resulting in a surface density of approximately 10000 resonance units (RU). The activated BinB could bind to BinA as 1:1 ratio (Figure 4-13). The further studies, mutated BinB will be tested binding to BinA.

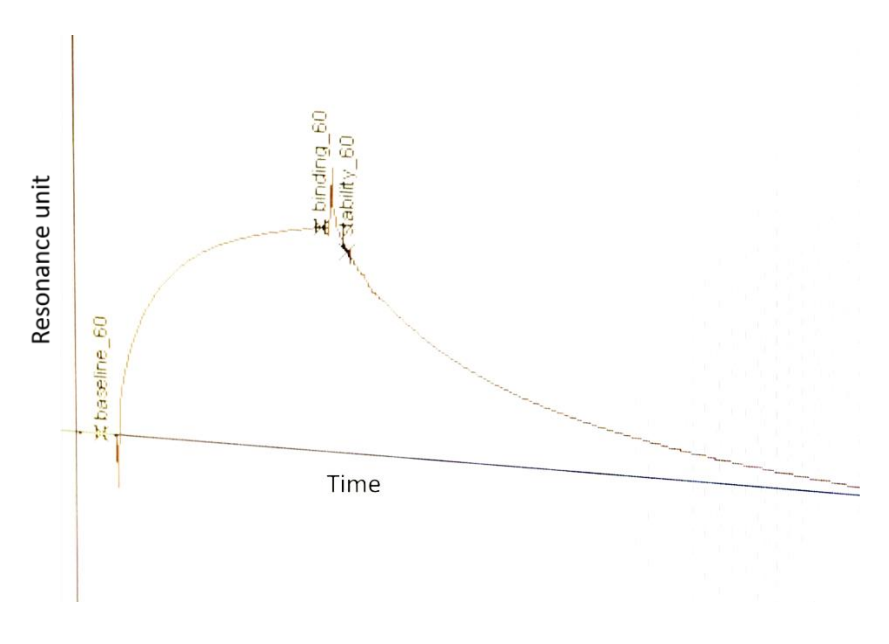


Figure 4-13 BinA and BinB interaction using Surface Plasmon Resonance (SPR)

4.8 Effect of histidine-tag on the tertiary structure of binary toxins

The tertiary conformation (folding state) of the binary toxin was analyzed by intrinsic fluorescence spectroscopy. The purified proteins of approximately 20 µg/ml were excited at 280 nm and fluorescence emission spectra were recorded from 300-550 nm. The highest emission spectrum of His-BinA was about 300 nm, whereas that of the activated BinA was at 326 nm. Similar to BinA, the highest emission spectrum of His-BinB was observed at about 324 nm and the highest intensity of activated BinB spectrum was at about 326nm (Figure 4-14). This result suggests that the three-dimensional conformations of both BinA and BinB were not significantly changed with histidine tagged at N-terminal end. On the contrary, the highest peak of both unfolded BinA and BinB proteins was detected at 350 nm. In comparison, no spectrum shift towards the wavelength 350 nm was observed for His- and activated-Bin toxins implying a properly folded structure. According to these results, the overall structure of His-BinA and His-BinB have no deleterious effect by histidine tagged sequence.

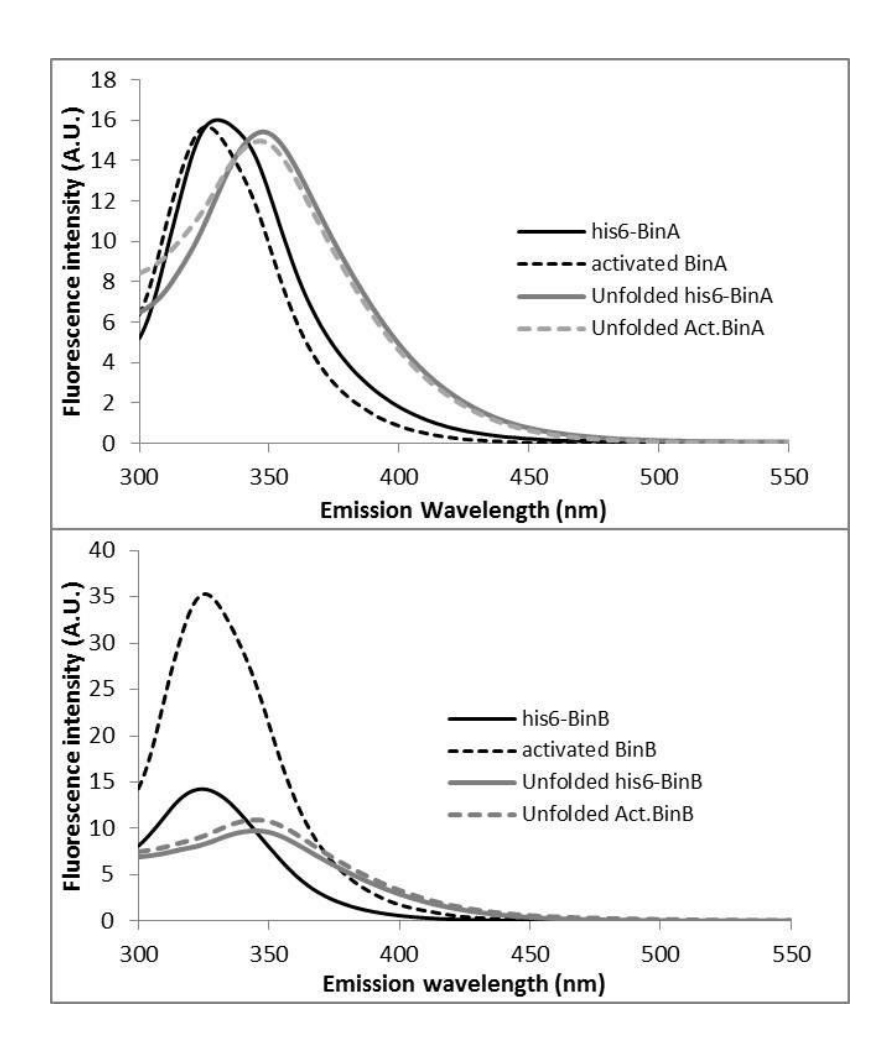


Figure 4-14 Intrinsic spectrum of folding structure of binary toxins. Fluorescence spectra of the binary toxin. The proteins were excited at 280 nm. The emission spectra were recorded from 300-550 nm. Upper panel and lower panel are the fluorescence spectra profiles of BinA and BinB, respectively.

4.9 Interaction of His-BinA and His-BinB with chelating Ni²⁺-lipid bilayers

The binary toxin (BinA and BinB) have been proposed to bind on target cell membranes via glycosylated proteins prior exerting its toxicity. However, a precise receptor has not been identified yet. To approach the binary toxins onto the lipid surface, DGS-NTA (Ni²⁺) lipid was included into the lipid bilayers for the binding of His-BinA and His-BinB. The phosphatidylcholine (POPC) bilayer plus 2% (mole) of DGS-NTA (Ni^{2+}) lipid $(Ni^{2+}-POPC)$ was successfully formed by mean of lipid vesicle fusion. The final ΔF and ΔD values of the lipid bilayer were about -25 Hz and 1.0x10⁻⁶, respectively. The lipid bilayer formation process of Ni²⁺-POPC resembled to the POPC although the maximum values of vesicle adsorption for Ni2+-POPC was less than the POPC. The protein attachment was initially determined for His-BinB at a protein concentration of 10 μ g/ml (0.2 μ M). Figure 3A shows unchanged Δ F and Δ D values implying no binding of His-BinB on the lipid bilayer surface. Although the protein concentration was increased to 50 µg/ml (1.0 µM) the binding remained undetected. A parallel binding study with POPC bilayers was carried out as a negative control. Moreover, nonspecific binding of Bin toxin was controlled by activated Bin toxin (His-tag was removed from protein molecule by protease). No detection of BinB binding might be explained by either a limitation of technique sensitivity (17.7 ng cm⁻² Hz⁻¹) or unsuitable lipid bilayer condition (e.g. lipid fluidity). Taking into account the molecular weight of the toxin, it is probable that the thermodynamic state of the lipid is responsible for the absence of binding events. Consequently, phosphatidylethanolamine (POPE) was mixed into the lipid bilayer (1:1 POPC/POPE) in order to mimic a mosquito cell membrane. In addition, the DGS-NTA(Ni2+) lipid amount was increased to 5% (mole) to overcome the limitation of mass detection (Δ F). The 5% Ni²⁺-POPC/POPE bilayer was successfully formed as POPC and 2% Ni²⁺-POPC. (Figure 4-15B revealed the binding of both His-BinA and His-BinB onto the Ni²⁺-POPC/POPE bilayer. On the contrary, no binding of the activated Bin toxin confirmed the specific binding of His-tagged and chelating Ni²⁺-ion. After 30 minutes of incubation, the total deposited mass of His-BinB (Δ F = -30.2 Hz) was higher than the mass detected for His-BinA (Δ F = -21.9 Hz) (decreasing of Δ F indicates to increasing of deposited mass). On the other hand, the Δ D values of His-BinA (1.9x10⁻⁶) and His-BinB (1.2x10⁻⁶) indicated non-significant changes in layer viscosity (i.e. a low value indicates a rigid layer while high value suggests a soft layer). The different Δ F between His-BinA and His-BinB might be supported by its molecular weight (MW), which the BinB (51 kDa) is heavy than the BinA molecule (42 kDa) [1]. Stable signals were observed with TBS rinsing. Interestingly, His-BinA (Δ F= -6.2 Hz) was detached from Ni^{2+} -ion ca. 72% of bound protein whereas ca. 18% was calculated for His-BinB (Δ F= -24.6 Hz). For the dissipation, the ΔD value of His-BinA slightly decreased reaching to the value of His-BinB (1.2x10⁻⁶). The ΔD value indicates the rigid nature of His-BinB/lipid layers (and transient adsorption of His-BinA). TBS-removing of unbound protein from the lipid surface could be taken into account for His-BinB. In contrast, His-BinA seemed to detach from Ni²⁺-ion by buffer rinsing, which contradicts to low dissociation constant (K_D) of 6XHis-Ni²⁺ binding (14x10⁻⁹ M) [18]. Similarly, His-BinB required a higher imidazole concentration (250 mM) than His-BinA (100 mM) for the purification step. These results indicate that the His-tagged of BinB chelates with Ni²⁺-ion stronger than His-BinA. Although the 3D-structure of BinA and BinB are similar (see Figure 1), but a distinct function has been proposed for the binary toxin. The N-terminal trefoil domain of binary toxin revealed the most different region of molecule. It is possible that the Ni²⁺-chelation efficiency of His-tagged BinA and BinB at N-terminus was different. Recently, the lipid membrane permeability assay showed that BinA had a higher ability of membrane disturbing than BinB. It is likely that BinA tends to interact with lipid membrane than BinB. This might change the overall structure of BinA and subsequently interfere his tag binding with Ni²⁺ -lipid bilayers.

After protein attachment, the interaction between BinA and BinB was further investigated. The interaction was particularly demonstrated for His-BinB and activated BinA according to the stable chelation of His-BinB. The BinA and BinB have been proposed to interact to each other because of co-internalization into the susceptible cells and co-crystallization evidences. Figure 3B shows neither activated BinA nor activated BinB interacted with its complementary protein as indicated by unchanged of ΔF and ΔD signals. This result suggests that a post-conformational change of BinB-receptor binding may be important for BinA-BinB interaction rather than protein docking on lipid surface. In addition, the detaching of His-tagged BinA or BinB by imidazole solution resulted in decreasing of the ΔF and ΔD values closing to the baseline (zero value). This implies no protein insertion of Bin toxins into the lipid bilayer. The higher affinity of His-BinB, in contrast with His-BinA, was confirmed by binding competition. The protein mixture solution of His-BinA and His-BinB (50 µg/ml of each, 1.0 µM of His-BinB and 1.2 µM of His-BinA) was incubated with Ni²+-POPC/POPE bilayer. A mixture of activated BinA and BinB solution was used as a negative control (Figure 4-16). The ΔF and ΔD values for protein-lipid binding were -35.1 Hz and 1.5x10-6, respectively. TBS rinsing removed 20% of bound protein (ΔF = -28.2 Hz). The results suggest that His-BinB has Ni²+-ion binding affinity stronger than His-BinA.

In the conclusion, the histidine tag has no effect on the folding structure of binary toxin. This provides the advantage for facilitating the protein purification. Moreover, the histidine tag associates the binding of binary toxin onto the Ni^{*}-lipid bilayer. His-BinB strongly binds to Ni^{2*}-lipid bilayer. In contrast, His-BinA was removed from the lipid surface with buffer rinsing. It seems that the histidine-Ni^{2*} binding of His-BinA was interfered due to the alteration of its structure during BinA approaching on lipid bilayer surface.

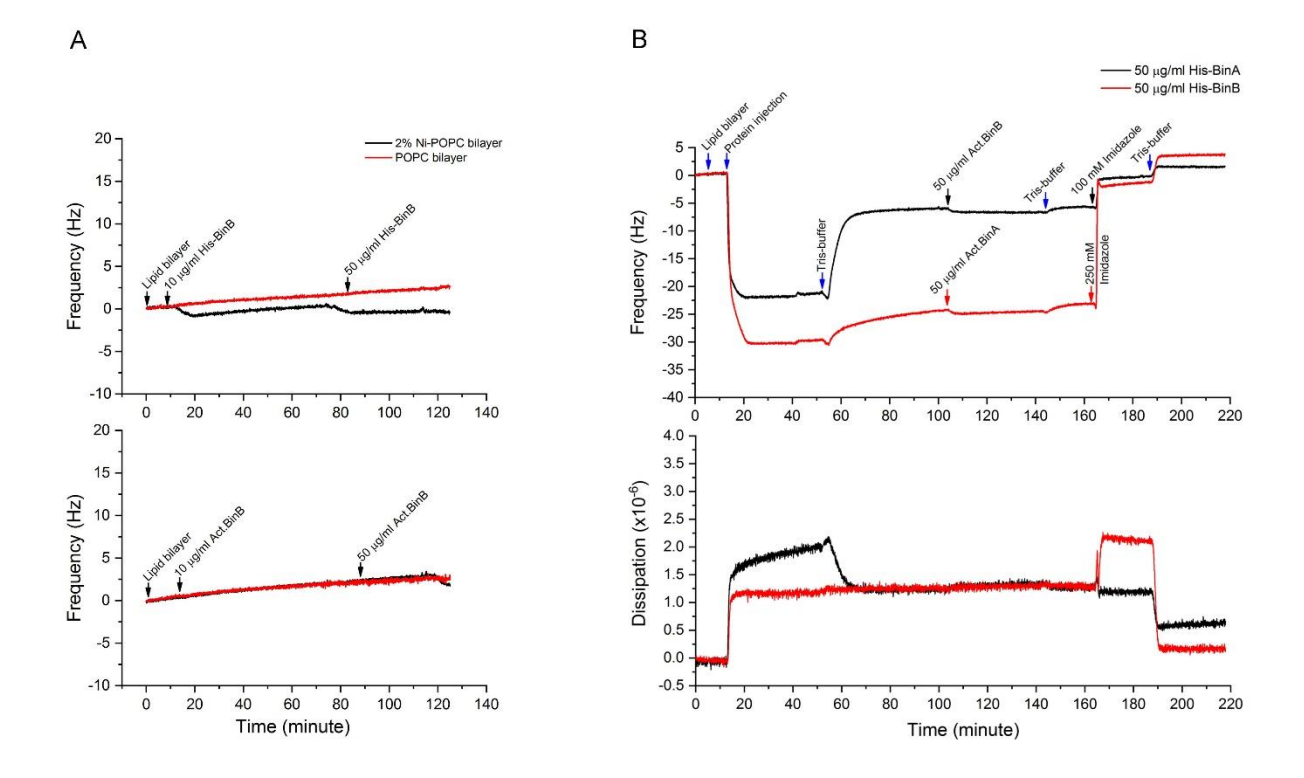


Figure 4-15. Interaction of binary toxins with Ni²⁺-lipid bilayers.

The lipid bilayers were formed via lipid vesicle fusion method. The lipid bilayer formation is indicated as zero value at the beginning of each plot. The solutions were injected into the QCM-D chamber at flow rate of 50 µl/min. The experiments were carried out at 25 °C. (A) 2% NTA(Ni²⁺)-POPC bilayer, and (B) 5% NTA(Ni²⁺)-POPC/POPE bilayer. The blue arrow indicates to the injection of same solution whereas the black and red arrows indicate to the injection of different solutions into the system of His-BinA and His-BinB, respectively.

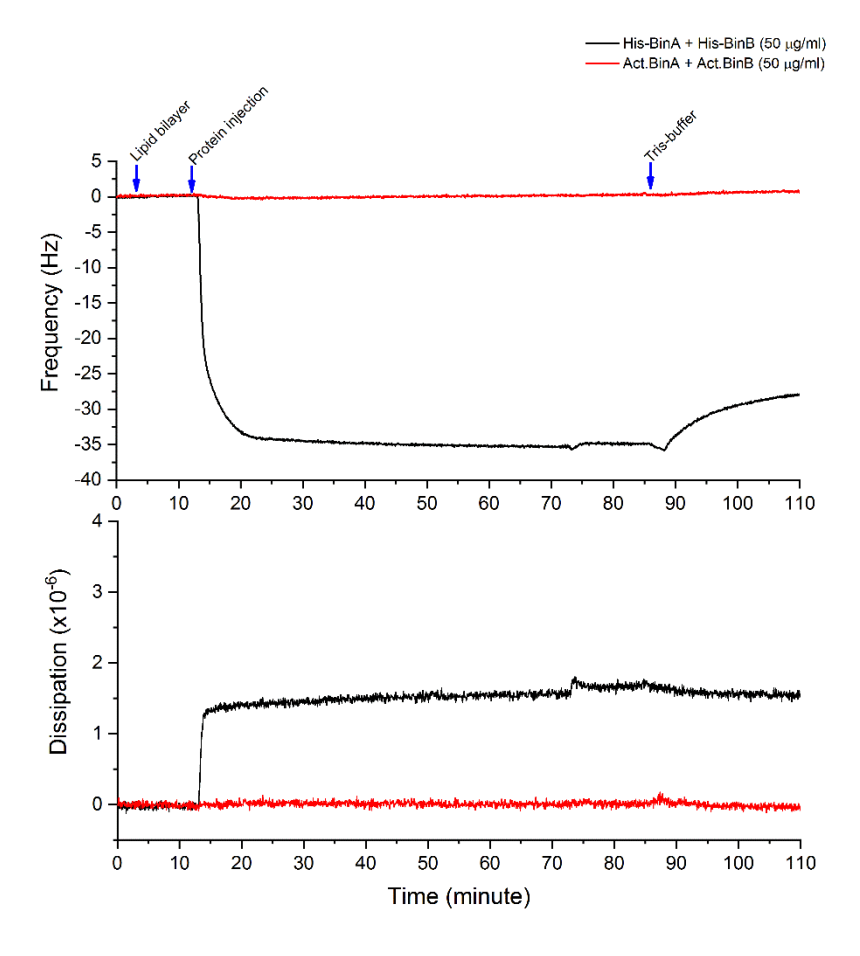


Figure 4-16. Competition binding of His-BinA and His-BinB onto Ni²⁺-lipid bilayer.

The protein solution containing 50 μ g/ml of each His-BinA and His-BinB was incubated with 5% NTA(Ni²⁺)-POPC/POPE bilayer for 70 minutes at 25 °C. After reaching a stable baseline, the systems were rinsed with TBS at the flow rate of 50 μ l/min.

4.10 Sugar recognition sites determined by crystal soaking experiment

The N-terminal domain of activated BinB structure is a lectin-like domain or sugar binding domain. So, we attempted to identify sugar binding sites by soaking BinB crystals with various sugars. The native crystal of activated BinB in a condition composed of 0.1 M Tris-HCl pH, 8.0, 0.2 M lithium sulfate and 12% (w/v) PEG 4000 was prepared for soaking with 15 sugars. The activated BinB crystals were soaked in reservoir solution containing 100 mM of each sugar for 1 hour and then the X-ray diffraction data sets were collected using an in-house X-ray machine with a cryocrystallographic condition of 25% glycerol and each sugar mixing in their mother liquor. The data sets were collected up to approximately 3 Å resolution. Electron density maps were calculated by molecular replacement method with MOLREP using the structure of activated BinB as a search model. The structure of the BinB-sugar complex reveals that two sugars, glucose and sucrose, could bind to BinB. The Fo-Fc electron density map reveals one possible site for glucose binding at the gamma motif of the N-terminal lectin domain. No additional sugar-binding site was observed at the other two motifs of this domain. Thereafter, glucose ligand coordinate obtained from the Protein Data Bank (BGC, beta-D-glucose) was manually fitted into the map. The refined model contains one glucose binding site where the electron density was clearly observed.

5. Conclusion

Despite mosquito larvicidal action of L. sphaericus binary toxin inside the Culex midgut cells as the primary target have been widely reported, there are no evidences of the binding residues of binary toxin on target cells. In this study, we have identified the importance amino acid residues on sugar binding domain of BinB that effect biological activity. Naturally, binary toxin is produced as a crystal toxin inside L. sphaericus during sporulation phase. Here, binary toxin was produced as soluble recombinant proteins by commercial E. coli BL21. However, this is confirmed by the larvicidal activity on target cells that these soluble recombinant binary toxins showed high toxicity to C. quinquefasciatus larvae with LC50 about 17 ng/ml that is in a range of previous report. Y72A and Y111A of BinB showed significantly reduced toxicity when compare with wild type protein. Binding assay showed that Y72A and Y111A of BinB reduced binding signal in mosquito larval gut by immunohistochemistry. To check interaction on membrane, the histidine-conjugated binary toxins were attached onto the lipid bilayer surface via Ni2+ chelating. Subsequently, the attachment was successful with Ni2+-POPC/POPE bilayer (mimic mosquito cell membrane) but not for Ni2+-POPC bilayer. However, unstable attachment was detected for His-BinA since bound protein could be removed by buffer rinsing. In contrast, His-BinB resisted to buffer rinsing until detaching by imidazole solution. The distinct N-terminal trefoil domain of binary toxin has been supposed to interfere the His-Ni²⁺ chelating of His-BinA. Moreover, structural conformational change during lipid membrane approaching may reduce the efficiency of Ni2+ binding of HisBinA. In the conclusion, the histidine tag has no effect on the folding structure of binary toxin. This provides the advantage for facilitating the protein purification. Moreover, the histidine tag associates the binding of binary toxin onto the Ni^{*}-lipid bilayer. His-BinB strongly binds to Ni^{2*}-lipid bilayer. In contrast, His-BinA was removed from the lipid surface with buffer rinsing. It seems that the histidine-Ni^{2*} binding of His-BinA was interfered due to the alteration of its structure during BinA approaching on lipid bilayer surface.

Output (Acknowledge the Thailand Research Fund)

International Journal Publication: Local conformations affect the histidine tag-Ni2+ binding affinity of BinA and BinB proteins. (2020) submit to Journal of AIMS Biophysics

National journal publication: Biological and Anti-cancer activity of Binary toxin from *Lysinibacillus* sphaericus, (2020) submit to Journal of the Medical Technologist Association of Thailand

Mosquito Larvicidal Binary Toxin from Lysinibacillus sphaericus: Structure and Application, วารสารวิทยาศาสตร์ บูรพา ปีที่ 23 (ฉบับที่ 3) กันยายน – ธันวาคม พ.ศ. 2561

International proceeding:

Srisucharitpanit K, Boonserm P, Srisaisup M. (2017) Role of selected polar amino acids in conserve putative transmembrane region of BinB from *Bacillus sphaericus*. In proceeding of the 6th Burapha University International Conference

6. เอกสารอ้างอิง

- 1. Baumann L, and P. Baumann. (1991) Effects of Components of the *Bacillus sphaericus* Toxin on Mosquito Larvae and Mosquito-Derived Tissue Culture-Grown Cells Current Microbiology 23: 51-57.
- 2. Berry C (2012) The bacterium, Lysinibacillus sphaericus, as an insect pathogen. J InvertebrPathol109: 1-10.
- 3. Boonserm P, Moonsom S, Boonchoy C, Promdonkoy B, Parthasarathy K & Torres J (2006) Association of the components of the binary toxin from *Bacillus sphaericus* in solution and with model lipid bilayers. Biochem.Biophys. Res. Commun. 342: 1273-1278.
- 4. Broadwell AH & Baumann P (1987) Proteolysis in the gut of mosquito larvae results in further activation of the *Bacillus sphaericus* toxin. Appl Environ Microbiol53: 1333-1337.
- 5. Carpusca I, Jank T &Aktories K (2006) *Bacillus sphaericus* mosquitocidal toxin (MTX) and pierisin: the enigmatic offspring from the family of ADP-ribosyltransferases. MolMicrobiol 62: 621-630.
- 6. Chapman HC (1974) Biological control of mosquito larvae. Annu Rev Entomol 19: 33-59.
- 7. Charles JF, Nielson-LeRoux C & Delecluse A (1996) *Bacillus sphaericus* toxins: molecular biology and mode of action. Annu Rev Entomol41: 451-472.
- 8. Cokmus C, Davidson EW & Cooper K (1997) Electrophysiological effects of *Bacillus sphaericus* binary toxin on cultured mosquito cells. J InvertebrPathol69: 197-204.
- 9. Cole AR, Gibert M, Popoff M, Moss DS, Titball RW &Basak AK (2004) *Clostridium perfringens* epsilon-toxin shows structural similarity to the pore-forming toxin aerolysin. Nat StructMolBiol11: 797-798.
- 10. Collier RJ (2001) Understanding the mode of action of diphtheria toxin: a perspective on progress during the 20th century. Toxicon39: 1793-1803.
- 11. Darboux I, Nielsen-LeRoux C, Charles JF &Pauron D (2001) The receptor of *Bacillus sphaericus* binary toxin in Culexpipiens (Diptera: Culicidae) midgut: molecular cloning and expression. Insect BiochemMolBiol31: 981-990.
- 12. Davidson EW (1988) Binding of the *Bacillus sphaericus* (Eubacteriales: Bacillaceae) toxin to midgut cells of mosquito (Diptera: Culicidae) larvae: relationship to host range. J Med Entomol25: 151-157.
- 13. Finney DJ (1971) Probit Analysis, 3rded. By D. J. Finney, Cambridge University Press, 32 E. 57th St., New York, Ny10022, 1971.. 1432-1432. American Pharmaceutical Association.
- 14. Kalfon A, Charles JF, Bourgouin C & de Barjac H (1984) Sporulation of *Bacillus sphaericus* 2297: an electron microscope study of crystal-like inclusion biogenesis and toxicity to mosquito larvae. J Gen Microbiol130: 893-900.
- 15. Nicolas L, LecroiseyA& Charles JF (1990) Role of the gut proteinases from mosquito larvae in the mechanism of action and the specificity of the *Bacillus sphaericus* toxin. Can J Microbiol36: 804-807.
- 16. Oei C, Hindley J & Berry C (1992) Binding of purified *Bacillus sphaericus* binary toxin and its deletion derivatives to *Culex quinquefasciatus* gut: elucidation of functional binding domains. J Gen Microbiol138: 1515-1526.
- 17. Parker MW, Buckley JT, Postma JP, Tucker AD, Leonard K, Pattus F &Tsernoglou D (1994) Structure of the Aeromonas toxin proaerolysin in its water-soluble and membrane-channel states. Nature 367: 292-295.
- 18. Pauchet Y, Luton F, Castella C, Charles JF, Romey G &Pauron D (2005) Effects of a mosquitocidal toxin on a mammalian epithelial cell line expressing its target receptor. Cell Microbiol7: 1335-1344.

- 19. Promdonkoy B, Promdonkoy P & Panyim S (2008) High-level expression in *Escherichia coli*, purification and mosquito-larvicidal activity of the binary toxin from *Bacillus sphaericus*. CurrMicrobiol57: 626-630.
- 20. Regis L, Silva-Filha MH, Nielsen-LeRoux C & Charles JF (2001) Bacteriological larvicides of dipteran disease vectors. Trends Parasitol17: 377-380.
- 21. Reinert DJ, Carpusca I, Aktories K & Schulz GE (2006) Structure of the mosquitocidal toxin from *Bacillus* sphaericus. J MolBiol357: 1226-1236.
- 22. Reithmeier RA (1995) Characterization and modeling of membrane proteins using sequence analysis. CurrOpinStructBiol5: 491-500.
- 23. Schwartz JL, Potvin L, Coux F, et al. (2001) Permeabilization of model lipid membranes by *Bacillus* sphaericus mosquitocidal binary toxin and its individual components. J. Membr. Biol. 184: 171-183.
- 24. Silva-Filha MH &Peixoto CA (2003) Immunocytochemical localization of the Bacillus sphaericus binary toxin components in *Culex quinquefasciatus* (Diptera:Culicidae) larvae midgut. Pesticide BiochemPhysiol77: 138-146.
- 25. Silva-Filha MH, Nielsen-LeRoux C & Charles JF (1999) Identification of the receptor for Bacillus sphaericus crystal toxin in the brush border membrane of the mosquito *Culex pipiens* (Diptera: Culicidae). Insect BiochemMolBiol29: 711-721.
- 26. Srisucharitpanit K, Inchana P, Rungrod A, Promdonkoy B &Boonserm P (2012) Expression and purification of the active soluble form of *Bacillus sphaericus* binary toxin for structural analysis. Protein ExprPurif82: 368-372
- 27. Srisucharitpanit K, Yao M, Promdonkoy B, Chimnaronk S, Tanaka I, Boonserm P. Crystal structure of BinB: A receptor binding component of the binary toxin from *Lysinibacillus sphaericus*. Proteins. 2014 Oct; 82(10):2703-12.
- 28. Yuan Z, Rang C, Maroun RC, et al. (2001) Identification and molecular structural prediction analysis of a toxicity determinant in the *Bacillus sphaericus* crystal larvicidal toxin. Eur J Biochem268: 2751-2760.
- 29. ทรัพย์อนันต์ วิเศษชาติ. 2553. การศึกษาโปรตีโอมจากเซลล์กระเพาะลูกน้ำยุงเมื่อได้รับโปรตีนสารพิษ Binary จากแบคทีเรีย Bacillus sphaericus. วิทยานิพนธ์ปริญญาโท. ภาควิชาเทคโนโลยีชีวภาพ คณะวิทยาศาสตร์และ เทคโนโลยี มหาวิทยาลัยธรรมศาสตร์.
- 30. Marheineke K, Grünewald S, Christie W, et al. (1998) Lipid composition of *Spodoptera frugiperda* (Sf9) and *Trichoplusia ni* (Tn) insect cells used for baculovirus infection. *FEBS Letters* 441: 49-52.
- 31. Knecht S, Ricklin D, Eberle AN, et al. (2009) Oligohis-tags: mechanisms of binding to Ni2+-NTA surfaces. Journal of Molecular Recognition 22: 270-279.
- 32. Chooduang S, Surya W, Torres J, et al. (2018) An aromatic cluster in *Lysinibacillus sphaericus* BinB involved in toxicity and proper in-membrane folding. *Arch Biochem Biophys* 660: 29-35.